Water Resources Research

RESEARCH ARTICLE
10.1029/2023WR035276

Evapotranspiration From Developed Land and Urban Watersheds in a Humid Subtropical Climate

Jeremy E. Diem[1], Dinah K. Carlton[2], and Luke A. Pangle[1]

[1]Georgia State University, Atlanta, GA, USA, [2]Nutter & Associates, Inc., Athens, GA, USA

Key Points:

- Evapotranspiration (ET) varies greatly among developed land-cover classes in a humid subtropical climate
- ET totals specific to land-cover classes aggregate to reliable estimates for urban watersheds
- The largest source of uncertainty for urban ET estimates is likely the magnitude of evaporation from impervious surfaces

Supporting Information:

Supporting Information may be found in the online version of this article.

Correspondence to:

J. E. Diem,
jdiem@gsu.edu

Citation:

Diem, J. E., Carlton, D. K., & Pangle, L. A. (2023). Evapotranspiration from developed land and urban watersheds in a humid subtropical climate. *Water Resources Research*, *59*, e2023WR035276. https://doi.org/10.1029/2023WR035276

Received 4 MAY 2023
Accepted 3 OCT 2023

Author Contributions:

Conceptualization: Jeremy E. Diem, Dinah K. Carlton, Luke A. Pangle
Data curation: Jeremy E. Diem
Formal analysis: Jeremy E. Diem, Dinah K. Carlton
Funding acquisition: Luke A. Pangle
Investigation: Jeremy E. Diem
Methodology: Jeremy E. Diem, Dinah K. Carlton, Luke A. Pangle
Project Administration: Luke A. Pangle
Resources: Jeremy E. Diem
Software: Jeremy E. Diem
Supervision: Jeremy E. Diem
Validation: Jeremy E. Diem
Visualization: Jeremy E. Diem

Abstract Urbanization introduces new and alters the existing hydrological processes. Projecting the direction and magnitude of change of evapotranspiration (ET), often a large existing process, in humid subtropical climates is difficult due to the lack of land-cover specific estimates of ET. This research aims to improve our fundamental understanding of ET in urban areas by focusing on ET specific to land-cover classes of the National Land Cover Database (NLCD). Using multiple physically based models along with ET from reference watersheds, this study estimates ET—within the Atlanta, GA, USA region—for NLCD classes. ET also is estimated for urban watersheds—both in the Atlanta region and in areas with humid subtropical climate types—for which published ET estimates exist. There are major differences in land cover among the four developed classes: high-intensity developed land is 92% impervious surfaces, while open-space developed land—the least intensively developed land—is only 8% impervious surfaces. Consequently, open-space developed land has an ET total that is over four times that of high-intensity developed land. Due to a high percentage of impervious cover and substantial evaporation of water from impervious surfaces throughout the year, there is little intra-annual variation in ET for the high-intensity developed class. The land-cover ET totals aggregate to reliable estimates for urban watersheds. The largest source of uncertainty for ET estimates in urban areas is likely the evaporation magnitude associated with impervious surfaces; therefore, more work is needed in determining those magnitudes for humid subtropical climates.

1. Introduction

Watersheds are becoming increasingly developed and will continue to do so in the future, thereby making the understanding of water flows in watersheds more difficult. At the global scale, urban land has been expanding at a rate of 5% per decade over the past several decades (Güneralp et al., 2020), and the amount of urban land could be up to six times larger in 2100 than the amount in 2000 (Gao & O'Neill, 2020). Urbanization introduces new pathways of water movement, including leakage from pressurized drinking-water pipes (Abd Rahman et al., 2018), exfiltration from sewer pipes (Rutsch et al., 2008), inflow and infiltration of water into sewer pipes (e.g., Bhaskar & Welty, 2012; Bhaskar et al., 2015; Pangle et al., 2022; K. Zhang & Parolari, 2022), effluent discharge by wastewater treatment plants (Townsend-Small et al., 2013), and increased water inputs by residential and commercial irrigation (Passarello et al., 2012). Urban areas also have increased runoff due to impervious surfaces and storm sewers (Booth & Jackson, 1997).

Similar to runoff, evapotranspiration (ET) is a hydrologic process affected by urbanization. ET is the combination of evaporative transfer of water from open water, foliar surfaces, non-vegetated surfaces, and transpiration through plant stomata (Thornthwaite, 1948). In humid regions, less vegetative cover in urban watersheds compared to rural watersheds presumably causes decreased ET (Bhaskar & Welty, 2012; Fang et al., 2020; Peters et al., 2011). In suburban areas in arid or Mediterranean climates, landscape irrigation causes urban ET to be larger than rural ET (Kokkonen et al., 2018; Oke, 1979). Urbanization can alter atmospheric processes (Arnfield, 2003), thereby impacting ET, which is positively correlated with temperature, net solar radiation, wind speed, and negatively correlated with relative humidity (Hamilton et al., 2018; Hao et al., 2018; Hogan et al., 2020; Thompson et al., 2011; Williams et al., 2012).

Urban ET has been measured and estimated using a variety of approaches. The most accurate way to directly measure ET is through eddy covariance towers (Scott, 2010), and the few applications of this method have been confined mostly to small, irrigated portions of urban/suburban areas in arid and Mediterranean climates (Grimmond & Oke, 1999a). A physically based model, the Penman-Monteith approach, is commonly used to model ET in many biomes (Allen et al., 1998), and its application has been extended to some urban areas (e.g.,

Writing – original draft: Jeremy E. Diem, Dinah K. Carlton, Luke A. Pangle

Fang et al., 2020; Grimmond & Oke, 1991; Gyamfi et al., 2016; Jia et al., 2001; Kokkonen et al., 2018). The water-budget approach produces an estimate of a long-term, annual estimate of ET of a watershed as the difference between inflows and outflows, but the accuracy depends on the accurate quantification of all non-ET terms (e.g., precipitation, water withdrawals) (Welty, 2009). This approach has been applied to urban watersheds in the northeastern United States (Claessens et al., 2006; Sloto & Buxton, 2005) and eastern Australia (Mitchell et al., 2003). Other ET-estimation methods used in urban areas include the following: (a) the surface energy balance method (i.e., ET is the residual term) in the south-central United States (Liu et al., 2010); (b) the Noah land-surface model (Ek et al., 2003) in the northeastern United States (Bhaskar & Welty, 2012); (c) upscaling in situ transpiration measurements and turfgrass ET in the western United States (Litvak et al., 2017); and (d) using regression models with biome-specific ET values as the predictand (Fang et al., 2015) to estimate ET for urban watersheds in the southeastern United States (Diem et al., 2022).

Based on the small number of studies (Bhaskar & Welty, 2012; Chen et al., 2022; Diem et al., 2022; Fang et al., 2020; Jia et al., 2001; Liu et al., 2010; Sloto & Buxton, 2005) providing urban ET information in humid subtropical climates, there is considerable disagreement in ET totals. Urbanization in these areas typically causes deforestation (Nagy & Lockaby, 2011) and thus should reduce ET of watersheds. With the exception of eddy-covariance studies, all approaches noted in the previous paragraph are used to produce ET estimates in humid temperate regions. The range in annual ET for watersheds is large (381 mm), and differences in land cover certainly are a major contributor to the disparity in ET totals. However, the difference in land cover between the urban watersheds in Baltimore, MD, USA (Bhaskar & Welty, 2012) and Atlanta, GA, USA (Diem et al., 2022) is not large, but the Atlanta ET totals are over twice as large. Another deficiency of the research is a lack of ET values for specific urban land-cover classes: only one study (Liu et al., 2010) provides those values. Improving our understanding of land-cover-specific ET may be a meaningful step toward resolving disparities in ET estimates across urban watersheds with similar climates.

This research aims to improve our fundamental understanding of ET in urban areas and to expand the geographic breadth of model-based estimates of ET in urban watersheds. The work is a novel contribution because of the focus on the little-studied humid subtropical climate and the examination of ET at the resolution of individual land-cover types (within pixels) comprising the urban landscape mosaic. The objectives of the study are (a) to estimate long-term ET for the land-cover classes of the National Land Cover Database (NLCD), (b) to estimate long-term ET for a variety of urban watersheds, and (c) compare the estimates for land-cover classes and urban watersheds with previously published estimates.

2. Study Region

The chosen watershed, the South River Watershed (SRW) located in the center of the Atlanta–Sandy Springs–Gainesville combined statistical area (CSA) in the southeastern United States, was an ideal locale for calculating ET totals specific to NLCD land-cover classes (Figure 1). The entire Atlanta CSA exists within the humid subtropical climate type, which is characterized by hot, humid summers and no seasonal differences in precipitation (Trewartha & Horn, 1980). The humid subtropical climate occurs across the globe (Beck et al., 2018), making the findings from this study useful for urbanizing areas in many countries. Two watersheds designated as reference watersheds (i.e., watersheds with minimal anthropogenic modifications) by the United States Geological Survey (USGS) exist in the Atlanta CSA, which can be used to produce baseline ET estimates. Those watersheds were Fausett Creek in the northern portion of the CSA and Falling Creek in the southern portion of the CSA.

3. Data

A variety of publicly available data were used, and those data included the following: (a) gridded land cover; (b) gridded percent developed imperviousness; (c) gridded percent tree canopy; (d) daily temperature, solar radiation, relative humidity, and atmospheric pressure at five weather stations; (e) hourly precipitation at one weather station; (f) gridded leaf-area index; (g) gridded monthly precipitation; and (h) daily stream discharge at 10 gauging stations. The data are summarized in Table S1 of the Supporting Information S1 and described in detail in the following paragraphs.

Gridded land-cover, developed-imperviousness, and tree-canopy data were acquired for multiple years within the 2001–2019 period. All data had a spatial resolution of 30 m and were obtained from the NLCD of the

10.1029/2023WR035276

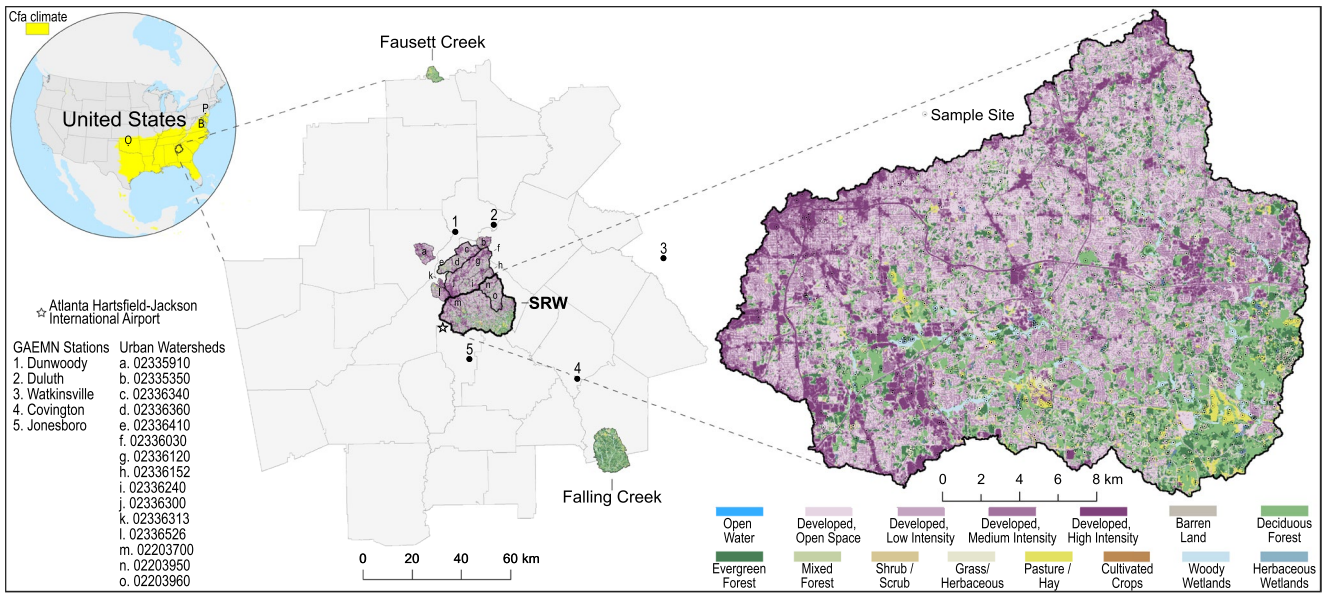

Figure 1. Location of the South River Watershed (SRW), two reference watersheds (Falling Creek and Fausett Creek), and 15 urban watersheds in the 30-county Atlanta-Gainesville-Sandy Springs combined statistical area within the southeastern United States. The 2019 land cover is shown for all watersheds. United States Geological Survey identification numbers are provided for the 15 urban watersheds, which are identified in Diem et al. (2022) and for which ET estimates exist. Also shown are the Atlanta airport weather station and Georgia Automated Environmental Monitoring (GAEMN) stations from which meteorological data were obtained. Shown on the small-scale map is the extent of the humid subtropical climate (Cfa) in the contiguous United States and the locations of Baltimore (B), Oklahoma City (O), and Philadelphia (P). Estimations of urban evapotranspiration (ET) by other studies have been made in and near those cities. Shown on the large-scale map of the SRW are the locations of the 620 pixels that were sampled.

Multi-Resolution Land Characteristics Consortium. The land-cover product had 15 classes for the Atlanta region (Figure 1), the imperviousness product had for each grid cell the percentage of developed surface that was impervious surfaces, and the tree-canopy product had for each grid cell the percentage that was tree canopy. Land-cover data were obtained for 2001, 2004, 2006, 2008, 2011, 2013, 2016, and 2019. Developed-imperviousness and tree-canopy data were obtained for 2016.

Meteorological data during 2001–2020 from six weather stations within and near the Atlanta region were used in the calculation of daily ET. Daily temperature, solar radiation, relative humidity, and atmospheric pressure were acquired from the Georgia Automated Environmental Network for five stations. All pixels in the SRW were given the same daily meteorological values, which were weighted values at the five weather stations. The weights were based on the inverse distance from the center of the SRW to each station. Hourly precipitation totals at Atlanta Hartsfield-Jackson International Airport were obtained from the National Oceanic and Atmospheric Administration.

Leaf-area index (LAI) data for the Atlanta region, which were needed to modify daily ET totals, were extracted from the MODIS MCD15A2H Leaf Area Index product (Myneni et al., 2015) for large ($\geq$1 km^2), homogeneous areas of deciduous forest, coniferous forest, and grassland (i.e., combined herbaceous and pasture/hay areas) in the Atlanta region from 2001 to 2020. The data had a spatial resolution of 500 m and a temporal resolution of 8 days. To downscale the data to daily values, all days within an 8-day period were given the value for the period.

Monthly precipitation and daily streamflow data were obtained for multiple reference watersheds so that ET totals could be derived using the water-budget approach. The two reference watersheds in the Atlanta region were Falling Creek and Fausett Creek (Figure 1), and eight watersheds near Baltimore and Philadelphia were used with respect to the urban watersheds in those locales (Figure 2). Data for watersheds near Baltimore and Philadelphia were needed to fulfill the third objective of the study, and details on how the data were used are provided in Section 4.4. Gridded monthly precipitation totals from PRISM (Parameter-elevation Regressions on Independent Slopes Model) were obtained from the PRISM Climate Group for 2001–2020. The spatial resolution of the data were 4 km. Daily mean stream discharge (in cfs) for all days during 2001–2020 was acquired from the USGS for the 10 gauges. The discharge values were converted to daily totals (in ft^3) and metric units (i.e., m^3) and then

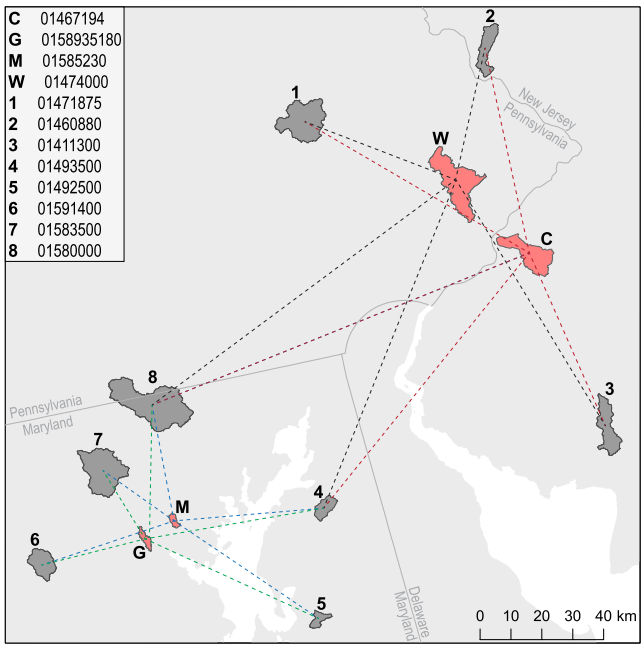

Figure 2. Locations of the two Baltimore urban watersheds (G and M), the two urban watersheds (C and W) in the Philadelphia region, and the eight reference watersheds. Reference watersheds associated with each urban watershed are indicated by dashed lines. C is the Cooper River watershed. G is the Gwynn's Run watershed. M is the Moore's Run watershed. W is the Wissahickon Creek watershed. The numbers with a leading zero are the United States Geology Survey identification numbers for the watersheds.

divided by watershed area (in m^2) to produce values in meters, subsequently converted millimeters. Using annual precipitation and streamflow totals, mean annual ET was estimated for 2001–2020.

4. Methods

The general procedures used to fulfill the objectives of the study are presented in Figure 3 and summarized below. To eventually have ET totals for land-cover classes and watersheds, ET totals for seven land-cover types (i.e., open water, impervious surfaces, deciduous forest, coniferous forest, mixed forest, shrubland, and grassland) were calculated. The developed imperviousness and tree-canopy data along with a sampling of land-cover classes in the SRW determined the proportion of each land-cover type with each land-cover class. The ET information for the land-cover types coupled with the class-specific area information of the types enabled the calculation of ET totals for each land-cover class. The class-specific totals were then used to estimate ET for urban watersheds in the Atlanta region, urban watersheds in Baltimore and near Philadelphia (see Figures 1 and 2), and developed land cover in Oklahoma City (see Figure 1).

4.1. Calculate ET Totals for Land-Cover Types

4.1.1. ET From Vegetation

A modified version of the Penman-Monteith equation was used to calculate daily ET totals from vegetation. The estimation of ET was calculated separately for deciduous forest, coniferous forest, mixed forest, shrubland, and grassland using the equation below, which is based on the equation in Grimmond and Oke (1991):

$$\mathrm{ET} = 0.035208\left(\frac{s(Q^* + Q_\mathrm{F} - \Delta Q_\mathrm{s}) + \frac{C_\mathrm{a}V}{r_\mathrm{a}}}{s + \gamma\left(1 + \frac{Br_\mathrm{s}}{r_\mathrm{a}}\right)}\right)A, \quad (1)$$

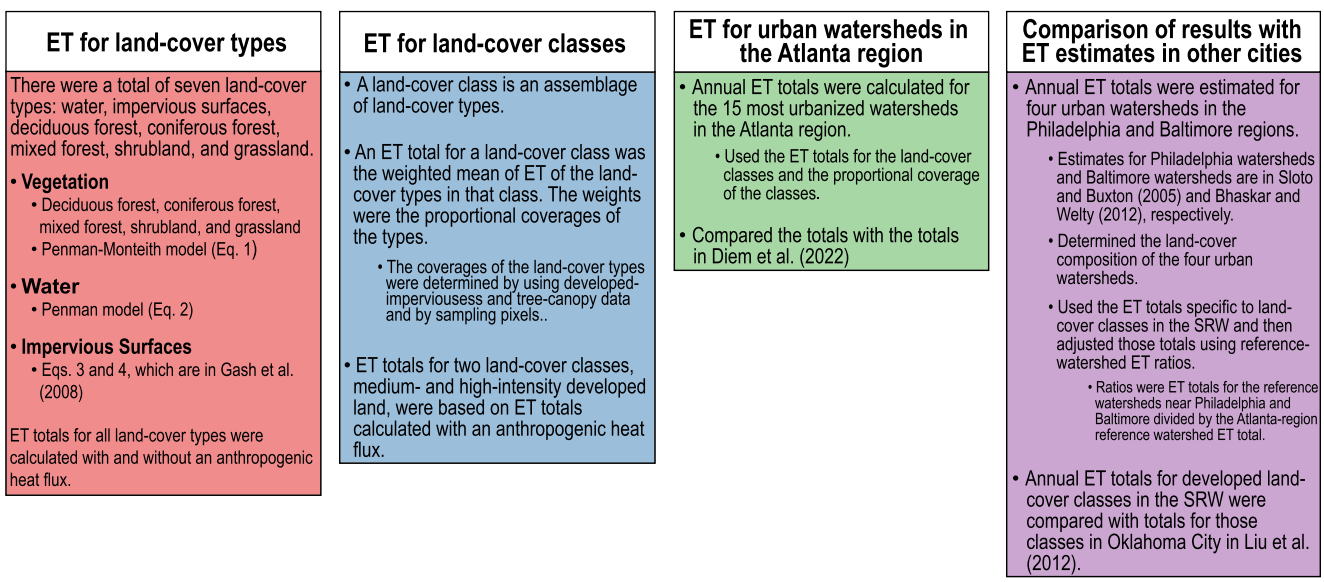

Figure 3. Summary of the processes involved in producing evapotranspiration (ET) totals for land-cover types and land-cover classes in the South River Watershed (the red and blue boxes) as well as the processes involved in taking the class-specific ET totals to the watershed level so that ET totals can be compared with totals from other studies.

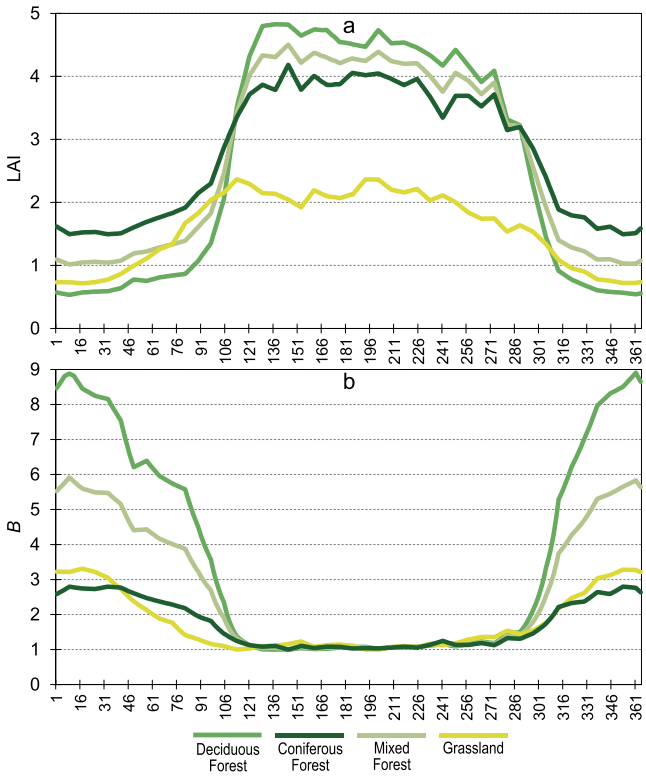

Figure 4. (a) Leaf area index (LAI) and (b) *B* values for each day of the year for the vegetated land-cover types. *B* is the inverse LAI for a specific day divided by the minimum daily inverse LAI. Mixed forest LAI was assumed to be the mean of deciduous forest and coniferous forest. The *B* values for coniferous forest were used for shrub, since most landscape shrubs in the Atlanta region are evergreen (Midcap et al., 2020).

where ET is daily evapotranspiration (mm), s is the slope of the saturation vapor pressure versus temperature curve (Pa °C^{-1}), Q^* *is* net radiation (W m^{-2}), Q_F is the anthropogenic heat flux (W m^{-2}), ΔQ_s is storage heat flux (W m^{-2}), C_a is the heat capacity of air (1,006 J m^{-3} °C), V is the vapor pressure deficit (Pa), γ is the psychometric constant (Pa °C^{-1}), r_a is aerodynamic resistance (s m^{-1}), r_s is the surface resistance (s m^{-1}), B is the leaf-area-adjustment factor for (r_s), and A is the ET-adjustment factor. B and A were new additions to Equation 1 that were devised for this project. Mean daily heat fluxes (Q_F) were calculated from hourly heat fluxes for Atlanta in the National Anthropogenic Heating Database (Arizona State University, 2023). The methodology for the heat fluxes is described in Sailor et al. (2015). The fluxes were converted from W m^{-2} to MJ m^{-2}. The daily values for Atlanta are provided in Table S2 of the Supporting Information S1. ET was calculated with and without Q_F. The equations for ΔQ_s, V, r_a, and r_s are S9, S11, S15, and S19, respectively, in Supporting Information S1.

The leaf-area-adjustment factor (B) was added because the Penman-Monteith equation in Grimmond and Oke (1991) does not account for changes in leaf area throughout the year. The initial r_s values, which were associated with the maximum biomass of a vegetation type, were adjusted to produce day-specific r_s values. B is the inverse LAI for a specific day divided by the minimum daily inverse LAI. Therefore, the minimum r_s values were assumed to occur during maximum LAI (Figure 4). B is similar in concept to scaling factors used in similar applications of the Penman-Monteith equation (e.g., Järvi et al., 2011).

The ET-adjustment factor (A) was needed in Equation 1, since the inclusion of B in the equation can yield annual ET totals that are too small or large. A for each vegetated land-cover type was the water-budget based annual ET estimate divided by the annual ET estimate derived from Equation 1 without the inclusion of A. Q_F was not included in Equation 1 when producing the ET totals that were compared with ET totals at the reference watersheds. All daily ET estimates were multiplied by the adjustment factor. Water-budget based annual ET totals for forest, shrubland, and grassland in the SRW were estimated using ET totals at the reference watersheds (Falling Creek and Fausett Creek) (Table 1). Since some studies have found forests to have larger ET than grasslands in the middle latitudes (e.g., L. Zhang et al., 2001) and other studies have found the opposite situation (e.g., Williams et al., 2012), annual ET totals for the vegetated land-cover types in the SRW were assumed to be the same as each other. The annual ET for vegetation in the SRW was the weighted mean of the annual ET at the two reference watersheds. The final weights were the mean of two sets of weights created using inverse-distance weighting: one set was derived from latitudinal differences between the reference watersheds and the SRW and the other set was derived from elevation differences. This ET total is referred to as the Atlanta-region reference watershed ET total in the remainder of the paper.

Table 1
Mean Annual Precipitation (P), Discharge (Q), and Evapotranspiration (ET) As Well As Latitude (in Degrees), Elevation (in m.a.s.l.), and ET Weights for the Two Reference Watersheds (Falling Creek and Fausett Creek) for 2001–2020

Watershed	*P*	*Q*	ET	Latitude	Elevation	ET weight
Falling Creek	1,223	236	987	33.17	160	0.64
Fausett Creek	1,461	522	939	34.58	486	0.36
SRW	N/A	N/A	N/A	33.70	272	N/A

Note. The ET weights are used to estimate ET at the South River Watershed (SRW). Also included is the latitude (in °) and elevation (in m a.s.l.) of the SRW. ET is *P* minus *Q*, and the three variables are in mm.

4.1.2. ET From Water

Daily ET totals from water were calculated using the Penman equation. The equation, as shown in McMahon et al. (2013), is as follows:

$$E = \left(\frac{\Delta}{\Delta+\gamma}\right)\left(\frac{R_n}{\lambda}\right) + \left(\frac{\gamma}{\Delta+\gamma}\right)E_a, \quad (2)$$

where E is the daily potential evaporation (mm day^{-1}) from a saturated surface, Δ is the slope of the relationship between vapor pressure and air temperature (kPa °C^{-1}), λ is the latent heat of vaporization (2.45 MJ kg^{-1}), R_n is net radiation over the evaporating surface (MJ m^{-2}), E_a is the evaporative component due to wind (mm day^{-1}), and γ is the psychrometric constant

(kPa °C^{-1}). R_n was calculated with and without the addition of Q_F. The equations for Δ, R_n, E_a, and γ are S1, S2, S14, and S23, respectively, in Supporting Information S1.

4.1.3. ET From Impervious Surfaces

Daily evaporation totals from impervious surfaces were estimated using daily precipitation totals, evaporation estimates, and the interception-loss model in Gash et al. (2008). Daily interception loss (i.e., evaporation) was calculated as follows:

$$I = m\sum_{j=1}^{m} P_{G,j} + n\left(P'_G - S\right) + \frac{\overline{E}}{\overline{R}}\sum_{j=1}^{n}\left(P_{G,j} - P'_G\right) + nS, \tag{3}$$

where m is the number of small storms in which the gross rainfall (P_G) is not sufficient to saturate the storage capacity (S) of the impervious surface and n is the number of storms in which it is. $\overline{E}/\overline{R}$ is the ratio of the mean evaporation and rainfall rates during saturated canopy conditions. P'_G is the rainfall that must fall below runoff starts. From Gash et al. (2008), 0.51 mm was used for S. The mean monthly values of $\overline{E}$, $\overline{R}$, and P'_G, were used for days in the corresponding month. $\overline{R}$ was calculated from hourly precipitation totals at Atlanta Hartsfield-Jackson International Airport from 2001 to 2020. $\overline{E}$ was calculated using Equation 2, and—within that equation—R_n was calculated with and without the addition of Q_F. P'_G was calculated as follows:

$$P'_G = -S\left(\frac{\overline{R}}{\overline{E}}\right)\ln\left(1 - \frac{\overline{E}}{\overline{R}}\right). \tag{4}$$

4.2. Calculate ET Totals for Land-Cover Classes

4.2.1. Land-Cover Composition of Pixels

The proportions of land-cover pixels that were forest (i.e., tree canopy) and developed imperviousness were determined for all pixels in the SRW that did not change land-cover class from 2001 to 2019. This subset of all pixels was chosen to eliminate any confounding effect of changes in land cover on estimated ET over the period of analysis. This procedure was performed for 479,701 pixels, which was 90% of all pixels in the watershed. If the total of forest and developed impervious exceeded 100%, developed impervious took precedence (i.e., impervious did not change and forest was reduced to 100% minus the percent developed imperviousness).

A random sampling of 620 pixels from 2019 was performed to determine the mean proportion of shrub, grass, wetland, and open water for each of the 14 land-cover classes in the SRW. Since the four developed classes were likely to be more heterogeneous than the other classes, 30 pixels within each developed class were selected at random and each pixel was divided into nine cells (i.e., each cell was 100 m^2). Using 2019 imagery in Google Earth Pro, the majority land cover (i.e., forest, impervious surface, shrub, grass, or water) was determined for each of the 270 cells for each developed class. For the remaining 10 undeveloped classes, 50 points were placed at random within each pixel of the classes and the land cover at the point was recorded.

The procedures described above produced proportions of the five land-cover types (i.e., open water, deciduous forest, coniferous forest, mixed forest, shrubland, and grassland) for pixels in the SRW. The sampling of land cover did not reveal specific forest types; therefore, the following was assumed: (a) the only forest in the deciduous-forest class was deciduous forest; (b) the only forest in the coniferous-forest class was coniferous forest; and (c) the only forest in the remaining classes was mixed forest. Each pixel had a specific land-cover class (e.g., low-intensity developed land). Therefore, the proportional coverage of the five land-cover types within a land-cover class was the mean of the values from the pixels within that land-cover class.

4.2.2. ET for Land-Cover Classes

ET for a land-cover class was the weighted mean of the ET totals from the five land-cover types (see Section 4.1), with the weights being the proportional coverages of the types. ET totals of land-cover types that were calculated using Q_F—which produced larger totals—were used for ET estimates of medium-intensity and high-intensity developed land. ET totals that were not calculated using Q_F were used for the other 12 land-cover classes.

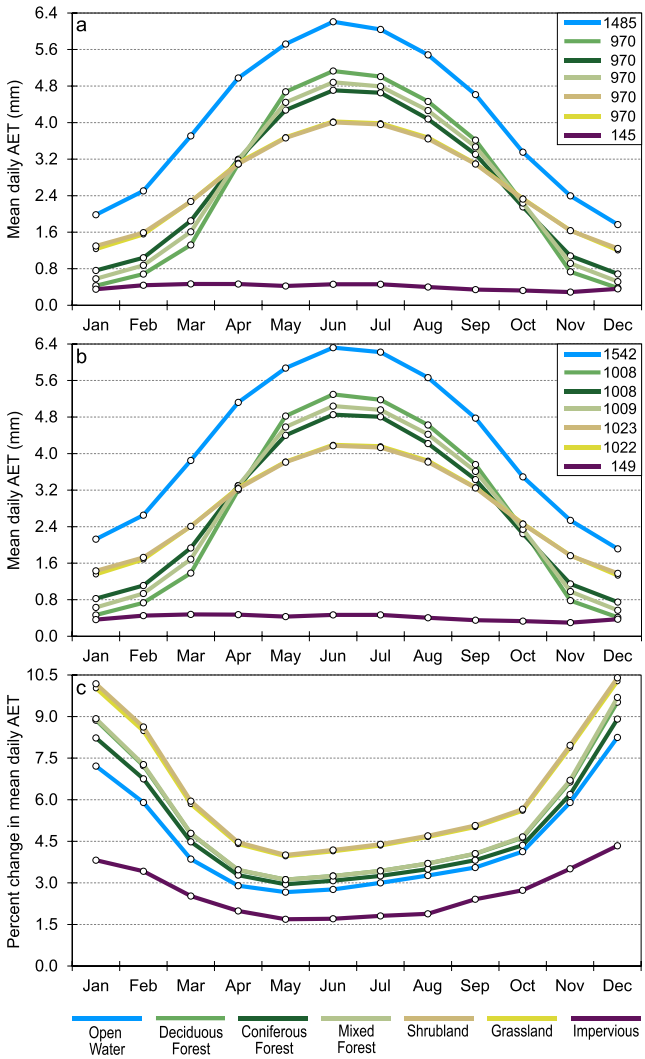

Figure 5. Mean daily values per month for the seven land-cover types of (a) evapotranspiration (ET) without the anthropogenic heat flux, (b) ET with the anthropogenic heat flux, and (c) percent change in daily ET when adding the anthropogenic heat flux. Annual ET totals are provided in the upper-right portions of panels (a) and (b)

4.3. ET for Urban Watersheds in the Atlanta Region

ET was calculated for the 15 most urbanized watersheds in the Atlanta region (Figure 1). Those watersheds had the largest urban score—derived from percent developed land, percent imperviousness, population density, and housing density—among 90 watersheds examined in Diem et al. (2022). Daily ET totals for the land-cover classes in the SRW were applied to the 15 urban watersheds. The underlying assumption in this study was that the actual compositions of surface types within a specific land-cover class are constant across watersheds, and that the watersheds have essentially identical meteorological conditions.

4.4. Comparison of Results With Other Urban ET Estimates in the Humid Subtropical Climate Type

Using the SRW-specific land-cover totals as well as ET totals from reference watersheds, ET totals were estimated for two urban watersheds in the Philadelphia, PA region and two urban watersheds in the city of Baltimore, MD (Figures 1 and 2) for which published ET totals exist. Sloto and Buxton (2005) use the water-budget approach to estimate annual ET for the Wissahickon Creek and Cooper River watersheds near Philadelphia; the time periods for the two watersheds are 1987–1998 and 1988–2002, respectively. Bhaskar and Welty (2012) use the Noah land-surface model to estimate annual ET for two watersheds in Baltimore; the time period is 2001–2009. The land cover for the watersheds was assumed to be the data in the NLCD land-cover product for 2001. The initial ET estimates for the urban watersheds near Philadelphia and in Baltimore derived from the SRW-based ET estimates for land-cover types had to be adjusted, because the SRW is at a much lower latitude (i.e., higher temperatures and more solar radiation) than Philadelphia and Baltimore and thus ET totals for the SRW are larger. Therefore, the initial ET estimates for the urban watersheds were downward adjusted by multiplying the totals by the ratio of the water-budget ET from reference watersheds near Philadelphia and Baltimore to the Atlanta-region reference watershed ET (i.e., the weighted mean of the Falling Creek and Fausett Creek ET totals) (Figure 2 and Table S3 in Supporting Information S1).

Direct comparisons of unadjusted ET totals from developed land in SRW were made with ET totals for developed land in the Oklahoma City, OK region (Figure 1). Liu et al. (2010) use the surface energy balance method to estimate annual ET totals for the four developed land-cover classes in the Oklahoma City region. The Oklahoma City region, which is located at the transition of a woodland ecoregion to the east and grassland ecoregion to the west (Woods et al., 2005), has a typical annual temperature for the Cfa climate type in the United States but receives much less precipitation than a typical Cfa locale (see Lindsey, 2021). As a result, urban areas in the region have larger irrigation-water use than do cooler or wetter locales (DeOreo et al., 2016; Opalinski et al., 2020). Therefore, it would not be reasonable to adjust class-specific ET totals in the SRW—using reference-watershed ET totals in the Atlanta region and Oklahoma City region—and then compare those ET totals with the ET totals calculated by Liu et al. (2010) for Oklahoma City.

5. Results

5.1. ET Totals of the Land-Cover Types

The annual ET totals of land-cover types in the SRW without impacts from anthropogenic heat ranged from 145 mm for impervious surfaces to 1,452 mm for open water (Figure 5a). The impervious evaporation total, which was derived from precipitation totals, was 12% of the mean annual precipitation total. As noted earlier,

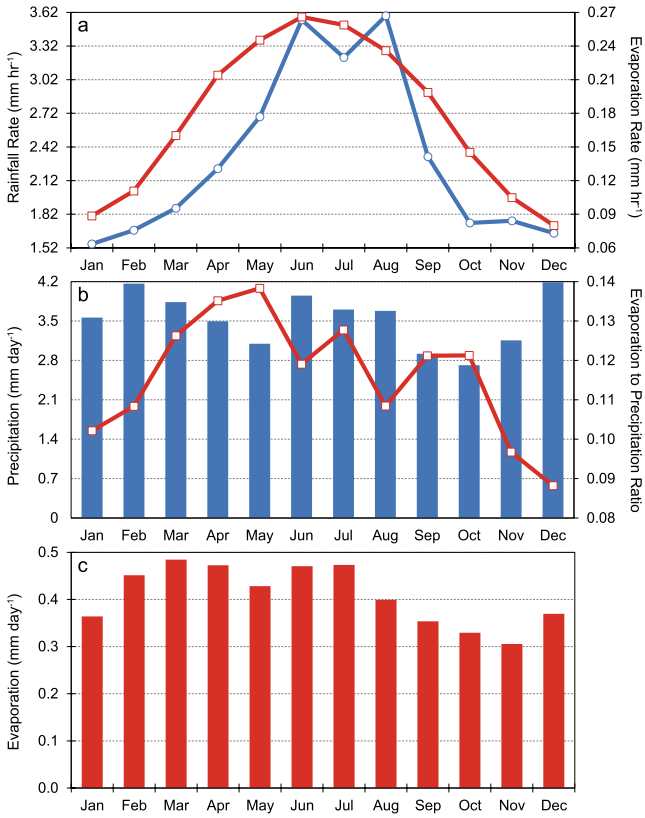

Figure 6. (a) Mean hourly rainfall rate (blue line) and evaporation rate (red line) per month. (b) Mean daily precipitation totals per month (blue bars) and monthly ratios of evaporation from an impervious surface to precipitation (red line). (c) Mean daily evaporation totals per month from an impervious surface.

the vegetated land-cover types (i.e., deciduous forest, coniferous forest, mixed forest, shrubland, and grassland) were all given an annual ET total of 970 mm.

ET for the vegetated land-cover types and water had the expected intra-annual variation of a maximum in summer and a minimum in winter (Figures 5a and 5b). The maximum and minimum ET months were June and December, respectively. Among the land-cover types, forests had the largest summer versus winter differences in ET, with deciduous forests having the largest difference.

There was substantial evaporation of precipitation from impervious surfaces during each month, with higher evaporation totals in spring and summer than in winter and autumn (Figure 6). There were distinct differences between winter and summer with respect to rainfall rates and evaporation rates, with summer having much higher rainfall and evaporation rates (Figure 6a). The ratio of evaporation to precipitation was highest during spring and lowest during winter (Figure 6b). Precipitation totals were higher in summer than in spring; therefore, total evaporation was highest during both spring and summer (Figure 6c).

The anthropogenic heat flux increased annual ET totals for all land-cover types, with the largest impact in winter (Figures 5b and 5c). Annual ET increased from 3% to 6%, with impervious surfaces and grassland/shrubland having the smallest increase and largest increase, respectively. Across the land-cover types, there were 8%, 4%, 3%, and 5% increases in winter, spring, summer, and autumn ET totals, respectively.

5.2. Composition of the Land-Cover Classes

Developed classes tended to be dominated by impervious cover while most of the remaining classes were predominantly forest cover (Figure 7). Among the developed classes, forest cover decreased from 63% to <1% and impervious cover increased from 8% to 92% when moving from the open-space developed class to the high-intensity developed class. The open-space developed class was mostly forest cover and had little impervious cover; therefore, that particular developed class was more similar to the forest classes than it was to the other developed classes. The forest classes, along with woody wetlands, were on average at least 85% forest cover. Grass was the dominant land cover of only two classes (pasture/hay and herbaceous); however, it did constitute at least 8% of the land cover of all the non-water classes.

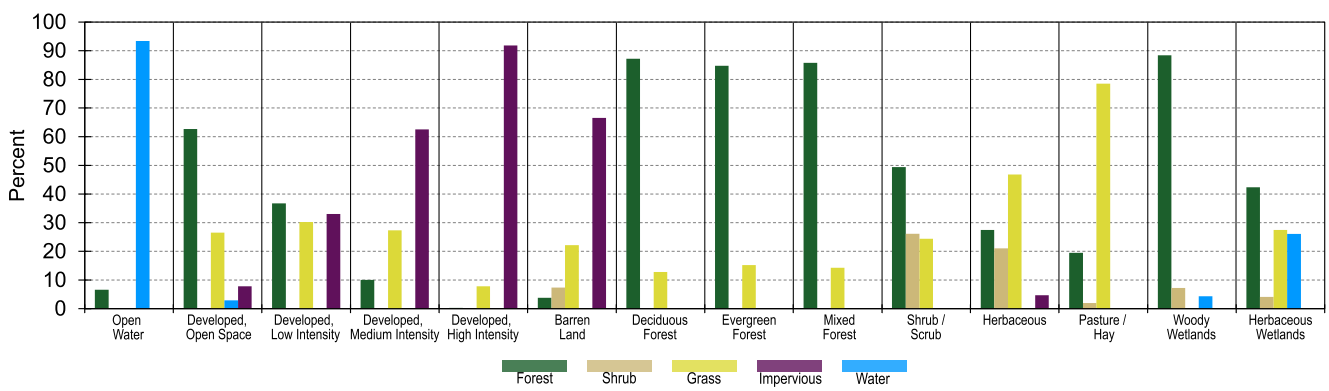

Figure 7. Mean percentages of land-cover types within each land-cover class. Mixed forest is the forest cover for all classes besides deciduous forest and coniferous forest.

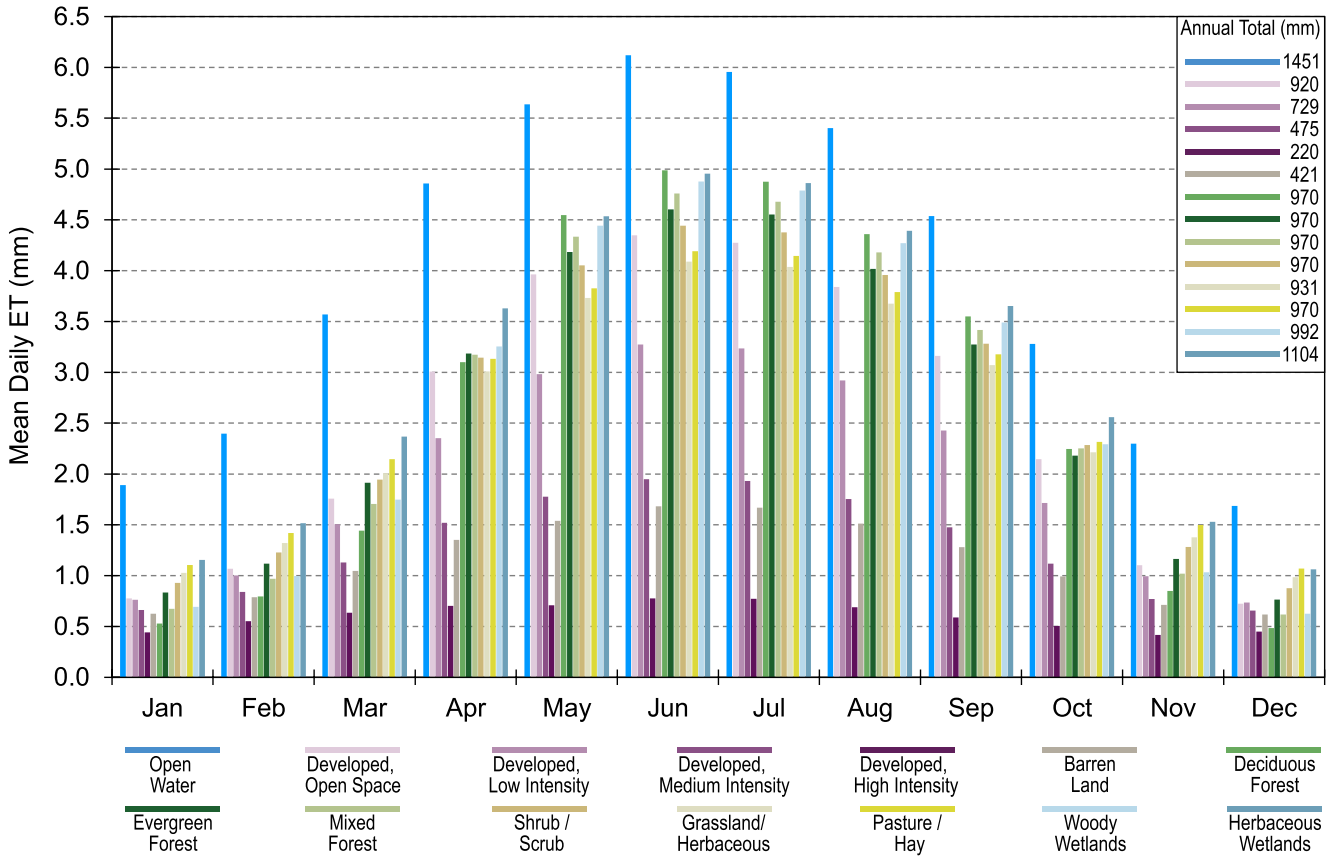

Figure 8. Mean daily evapotranspiration (ET) totals per month for the 14 land-cover classes in the South River Watershed.

5.3. ET Totals of the Land-Cover Classes

Annual ET totals for the 14 land-cover classes ranged from 241 mm to 1,451 mm (Figure 8). The forest and pasture/hay classes, which did not have any impervious surfaces or water, had 970 mm as the ET total, which was the weighted mean of the ET totals of the two reference watersheds. Undeveloped classes with some impervious cover, such as barren and grassland/herbaceous, had totals less than 970 mm, while undeveloped classes with a mixture of vegetation and water had totals exceeding 970 mm. The four developed classes (i.e., open-space developed, low-intensity developed, medium-intensity developed, and high-intensity developed) had totals of 922 mm, 737 mm, 489 mm, and 241 mm, respectively. As noted in Section 5.2, the open-space developed class was mostly forest; as a result, it had a relatively large ET total.

While all land-cover classes had a maximum ET in June and most classes had a minimum ET in December (Figure 8), there were considerable differences in intra-annual variability among the classes (Figure 9). Medium-intensity developed, high-intensity developed, and barren land, which were the three classes with the largest proportions of impervious surfaces, had the smallest coefficients of variation, while deciduous forest, mixed forest, and woody wetlands had the largest coefficients of variation (Figure 9). Because of the elevated winter ET resulting from evaporation from impervious surfaces and to a lesser degree enhanced ET from the anthropogenic heat flux, the developed classes—with the exception of high-intensity developed land—likely had more winter-season ET than did deciduous forest, mixed forest, and woody wetland.

5.4. ET Totals for Urbanized Watersheds

The ET totals for the 15 most urbanized watersheds in the Atlanta region were slightly less than the totals for those same watersheds in Diem et al. (2022) (Figure 10). The watersheds on average were ~85% developed, with little difference in coverage among the developed classes (Figure S1 in Supporting Information S1). The mean ET total from this study was 685 mm, which was 54 mm (~7%) smaller than the mean total in Diem et al. (2022).

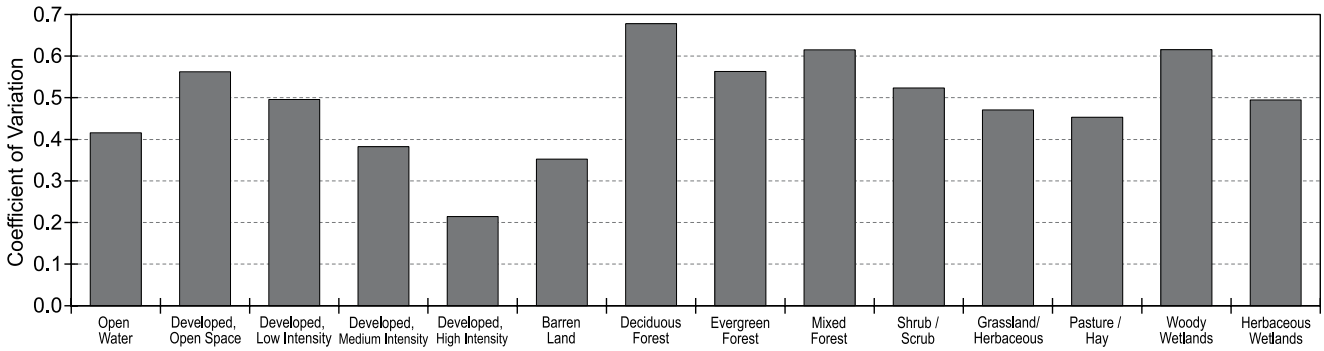

Figure 9. Coefficients of variation of daily evapotranspiration (ET) for the 14 land-cover classes in the South River Watershed.

The difference in ET totals between the two studies was highest for watersheds with the smallest ET totals (i.e., the largest difference was for watersheds with the highest percentage of impervious cover). The reasons for the differences in ET totals between the studies are presented in Section 6.1.

5.5. Applicability of Results to Other Areas

The ET values specific to land-cover classes in the SRW produced ET totals for urban watersheds near Philadelphia that were similar to published totals but produced much higher ET totals for urban Baltimore watersheds than the published totals for those watersheds (Table 2). The Cooper River watershed, located to the east of Philadelphia, was ~78% developed, with low-intensity developed land as the most prevalent land cover (Figure S1 in Supporting Information S1). The Wissahickon Creek watershed, located to the northwest of Philadelphia, was ~66% developed, with open-space developed land the most prevalent land cover (Figure S1 in Supporting Information S1). The estimated ET totals from this study for the Cooper River watershed and Wissahickon Creek watershed, were slightly smaller than (4%) and larger than (13%), respectively, than the published totals. The Baltimore watersheds were ~97% developed, with low-intensity developed land as the most prevalent land cover. The mean estimated ET total for the Baltimore watersheds was 525 mm, which was 46% larger than the published total. Individual values for the Baltimore watersheds are not presented, because only a mean total for the two Baltimore watersheds was provided in Bhaskar and Welty (2012).

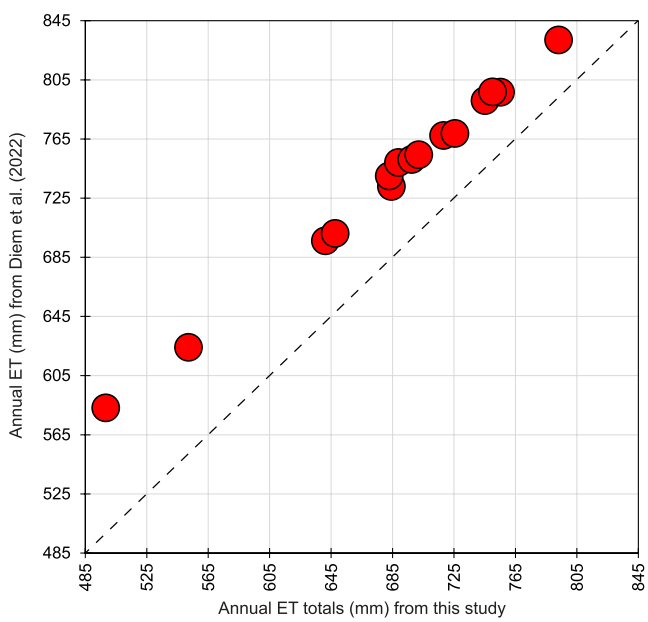

Figure 10. Scatter plot of urban-watershed evapotranspiration (ET) totals from Diem et al. (2022) versus ET totals from this study. All markers are to the left of the dashed line, thereby showing that all 15 ET totals in this study are smaller than the ET totals in Diem et al. (2022).

The ET totals for the four developed classes in the SRW had much more variation than the totals for the developed classes produced for the Oklahoma City region. The range in ET totals for the SRW was 220–920 mm, while the range for Oklahoma City was 657–778 mm. The percent difference between the ET totals from this study and the ET totals from the Oklahoma City study for open-space developed, low-intensity developed, medium-intensity developed, and high-intensity developed were 18%, 6%, −30%, and −66%. Therefore, compared to the results for Oklahoma City, this study had moderately higher ET totals for the open-space developed and low-intensity developed classes, moderately lower ET totals for the medium-intensity developed class, and substantially lower ET totals for the high-intensity developed class.

6. Discussion

6.1. ET Estimates Specific to Land Cover Inform Temporal and Cross-Study Contrasts in Urban ET

Rural land converted to medium- and high-intensity developed causes a much larger decrease in ET compared to the conversion of that cover type to open-space and low-intensity developed land. For example, converting forest land to open-space developed land, which is only 8% impervious surfaces, reduces ET by only 6%, while converting forest land to high-intensity

Table 2
Annual Evapotranspiration (ET) Information for the Two Urban Watersheds in Baltimore (B) in Bhaskar and Welty (2012) and the Cooper River (C) and Wissahickon Creek (W) Watersheds in Sloto and Buxton (2005)

	B	C	W
Unadjusted ET	647	741	850
Reference watershed ET	788	772	756
Reference watershed ratio	0.812	0.795	0.779
Adjusted ET	525	590	663
Published ET	360	613	587
ET percent difference	46	−4	13

Note. Unadjusted ET is the ET produced using the SRW-specific land-cover values. Reference watershed ET is the ET produced by using the water-budget approach at nearby reference watersheds. Reference watershed ratio is the ratio of the reference watershed ET to the SRW reference ET (i.e., 970 mm). Adjusted ET is the unadjusted ET multiplied by the reference watershed ratio. Published ET is the value in the aforementioned studies. ET percent difference is the adjusted ET total in this study compared with the published ET total. All ET totals are in mm.

developed land, which is 92% impervious surfaces, reduces ET by 78%. Therefore, it is important to examine the four developed land-cover classes separately when assessing impacts of development on ET.

Compared to rural areas, urban areas have lower ET in summer and tend to have higher ET in winter, thereby resulting in reduced intra-annual variability in ET in urban areas. This reduced intra-annual variability also has been found for multiple streamflow variables in urban watersheds (Bhaskar & Welty, 2012; Diem et al., 2021). Urban areas have relatively high ET totals in winter resulting from evaporation from a relatively large coverage of impervious surfaces and also from the anthropogenic heat flux enhancing ET from vegetated land cover. There is substantial winter precipitation in the Atlanta region, and in most other locales with humid subtropical climates, and is highly likely that at least 10% of precipitation that falls on impervious surfaces is evaporated. Urban areas have relatively low ET totals in summer, which is the peak season for ET, resulting from much less vegetative cover than rural areas.

The main reason this study has slightly smaller ET totals—compared to those in Diem et al. (2022)—for urban watersheds in the Atlanta region is much smaller estimates of evaporation from impervious surfaces. The evaporation to precipitation ratio used in Diem et al. (2022) is 0.20 and the mean annual precipitation total (for 2013–2020) is 1,447 mm. The ratio is the mean of observed ratios, which range from 0.10 to 0.38, provided in Cohard et al. (2018), Ragab, Bromley, et al. (2003), Ragab, Rosier, et al. (2003), Ramier et al. (2004), and Ramier et al. (2011). The mean evaporation to precipitation ratio in this study is 0.12 and the mean annual precipitation total is 1,294 mm. The total annual evaporation from an impervious surface would be 290 and 155 mm in Diem et al. (2022) and this study, respectively. The mean proportion of the urban watersheds that are impervious surfaces is 0.38; therefore, the mean impervious evaporation total from urban watersheds would be 111 and 59 mm in Diem et al. (2022) and this study, respectively. This 52 mm difference in evaporation almost exactly matches the 54 mm difference in mean ET for urban watersheds in the two studies.

6.2. ET Results for the Atlanta Region Are Applicable to Other Locales With Humid Subtropical Climates

ET results in this study transfer well to urban watersheds in the Philadelphia region, which is on the far northern edge of the humid subtropical climate type. ET totals of the two urban watersheds in the Philadelphia region are estimated using a detailed water budget, and the mean total for the two watersheds is 600 mm (Sloto & Buxton, 2005). Using differences in reference watershed ET totals between Atlanta and Philadelphia to modify the Atlanta-developed, land-cover specific values results in mean annual ET estimates of 630 mm at the Philadelphia watersheds. This is only a 9% difference in ET between the two approaches.

The urban ET totals from this study have magnitudes that are between estimated totals for Baltimore and Oklahoma City, which are dramatically different and appear to be underestimates and overestimates, respectively. The ET totals for the Baltimore watersheds in Bhaskar and Welty (2012) is 360 mm, which is 31% smaller than the ET total (525 mm) for those watersheds calculated with the land-cover and reference-watershed data and in this study. Based on the land-cover composition of the land-cover classes in the Atlanta region (Figure 7) and the land-cover of the Baltimore watersheds, it is assumed that the Baltimore watersheds are ∼60% vegetated. Since nearby reference watersheds have annual ET totals of ∼790 mm, urban ET could be as high as 470 mm without even accounting for evaporation from impervious surfaces. There does exist the possibility, however, that using the Atlanta-derived composition of the land-cover classes for Baltimore leads to overestimates of vegetation cover in Baltimore and thus overestimates of ET. The ET totals in Liu et al. (2010) for medium-intensity developed land and high-intensity developed land, which are 683 and 657 mm, respectively, seem high given that those two land-cover types are likely only 37% and 8% vegetated, respectively. The ET totals for those two classes in this study are on average 48% smaller. However, since there is substantial irrigation in the south-central United States (e.g., DeOreo et al., 2016; Opalinski et al., 2020) and the impact of residential and commercial irrigation

on ET for intensively developed areas is disproportionate and poorly constrained (e.g., Kokkonen et al., 2018), it may not be appropriate to transfer Atlanta-based results to locales such as Oklahoma City.

6.3. There Should Be Substantial Uncertainty in Urban ET Totals

There is substantial uncertainty in ET from vegetation. The uncertainty is likely at least 19%, which is the mean uncertainty of ET for small agricultural watersheds throughout the United States (Baffaut et al., 2020). It has been assumed in this study that urban vegetation is nearly identical to vegetation in rural watersheds, with the only difference being urban vegetation having ∼5% more annual ET resulting from the anthropogenic heat flux. But additional factors noted in Winbourne et al. (2020)—such as differences between urban and rural locales with respect to ambient carbon-dioxide concentrations, nutrient availability, growing-season length, light availability, exposure to invasive pests, and rooting-space restrictions—can make urban-vegetation ET differ from rural-vegetation ET.

There might be more uncertainty for grass than trees. The main reason for the increased uncertainty is that the reference watersheds, which were used to establish the annual ET totals for vegetation, are >83% forests and <15% grasslands. Therefore, the reference watersheds appear to be much better suited for estimating tree ET compared to grass ET. In addition, it is assumed in this study that forests and grasslands have the same annual ET, but—based on the mean annual precipitation total (∼1,300 mm) for the Atlanta region and numerical relationships between annual ET and annual precipitation for forested and grassland catchments in L. Zhang et al. (2001)—grasslands in the Atlanta region might have ∼30% less ET than forests. This decreased ET for grass is due in part to the relatively deep roots of trees and thus an ability to access soil moisture from greater depths compared to grass in water-deficit periods (e.g., Hodnett et al., 1995). Nevertheless, residents and land managers in the Atlanta region respond to the typical summer water deficit by applying ∼100 mm of irrigation water to landscapes (DeOreo et al., 2016; Diem et al., 2022).

It could be argued that there is even more uncertainty for ET from impervious surfaces than for ET from urban vegetation. As land becomes more developed there is more impervious cover and thus presumably more uncertainty in ET, since—as noted in previous sections—impervious evaporation to precipitation ratios from observational studies (Cohard et al., 2018; Ragab, Bromley, et al., 2003; Ragab, Rosier, et al., 2003; Ramier et al., 2004, 2011), all of which have been conducted in locales with temperate oceanic climates, range from 0.10 to 0.38. The ratio found in this study using the Gash et al. (2008) model is 0.12 and is thus at the lower end of the ratios from the observational studies. The evaporation totals from impervious surfaces in this study may be highly accurate or they may be several times smaller than actual totals.

7. Conclusions

This study has shown that ET varies considerably among the various land-cover classes, especially among developed (i.e., urban) classes, in a humid subtropical climate. All land-cover classes are comprised of multiple land-cover types. The annual ET totals of land-cover types ranged from 145 mm for impervious surfaces in rural areas to 1,542 mm for open water in urban areas. Land cover classified as developed tended to be dominated by impervious cover while many of the remaining classes were predominantly covered by forest. Annual ET totals for the 14 land-cover classes ranged from 241 mm for high-intensity developed land to 1,451 mm for water. High-intensity developed land was 92% impervious surfaces, while open-space developed land—the least intensively developed land—was only 8% impervious surfaces. As a result, open-space developed land had an ET total (920 mm) that was over four times that of high-intensity developed land. Due to a high percentage of impervious cover and substantial evaporation of water from impervious surfaces throughout the year, there was little intra-annual variation in ET for the high-intensity developed class. The results in this study, when applied to urban watersheds in the Atlanta region, matched results from a previous study, with the differences explained mostly by different magnitudes of evaporation from impervious surfaces between the two studies. The ET totals specific to land-cover classes also produced for urban watersheds in another locale results similar to those in another study where the water-budget approach was used to estimate ET. A large source of uncertainty for ET estimates in urban areas was likely the evaporation magnitude associated with impervious surfaces. Quantification of evaporation rates from impervious surfaces—considering diversity in their composition, roughness, slopes, and local meteorological conditions—represents an important knowledge gap in urban-watershed hydrology that should motivate future empirical studies.

Conflict of Interest

The authors declare no conflicts of interest relevant to this study.

Data Availability Statement

Land-cover and evapotranspiration data sets produced in this study are available in Diem (2023).

Acknowledgments
This work was supported by the National Science Foundation (Grant 1853809).

References

Abd Rahman, N., Muhammad, N. S., & Wan Mohtar, W. H. M. (2018). Evolution of research on water leakage control strategies: Where are we now? *Urban Water Journal*, *15*(8), 812–826. https://doi.org/10.1080/1573062X.2018.1547773

Allen, R. G., Pereira, L. S., Raes, D., & Smith, M. (1998). *Crop evapotranspiration – Guidelines for computing crop water requirements*. FAO Irrigation and drainage paper 56. Food and Agriculture Organization. Retrieved from https://www.fao.org/3/x0490e/x0490e00.htm

Arizona State University. (2023). National anthropogenic heating database [Dataset]. Retrieved from https://sgsup.asu.edu/national-anthropogenic-heating-database

Arnfield, A. J. (2003). Two decades of urban climate research: A review of turbulence, exchanges of energy and water, and the urban heat island. *International Journal of Climatology*, *23*(1), 1–26. https://doi.org/10.1002/joc.859

Baffaut, C., Baker, J. M., Biederman, J. A., Bosch, D. D., Brooks, E. S., Buda, A. R., et al. (2020). Comparative analysis of water budgets across the U.S. long-term agroecosystem research network. *Journal of Hydrology*, *588*, 125021. https://doi.org/10.1016/j.jhydrol.2020.125021

Beck, H. E., Zimmermann, N. E., McVicar, T. R., Vergopolan, N., Berg, A., & Wood, E. F. (2018). Present and future Köppen-Geiger climate classification maps at 1-km resolution. *Scientific Data*, *5*(1), 180214. https://doi.org/10.1038/sdata.2018.214

Bhaskar, A. S., & Welty, C. (2012). Water balances along an urban-to-rural gradient of metropolitan Baltimore, 2001–2009. *Environmental and Engineering Geoscience*, *18*(1), 37–50. https://doi.org/10.2113/gseegeosci.18.1.37

Bhaskar, A. S., Welty, C., Maxwell, R. M., & Miller, A. J. (2015). Untangling the effects of urban development on subsurface storage in Baltimore. *Water Resources Research*, *51*(2), 1158–1181. https://doi.org/10.1002/2014WR016039

Booth, D. B., & Jackson, C. R. (1997). Urbanization of aquatic systems: Degradation thresholds, stormwater detection, and the limits of mitigation. *Journal of the American Water Resources Association*, *33*(5), 1077–1090. https://doi.org/10.1111/j.1752-1688.1997.tb04126.x

Chen, J., Bu, J., Su, Y., Yuan, M., Cao, K., & Gao, Y. (2022). Urban evapotranspiration estimation based on anthropogenic activities and modified Penman-Monteith model. *Journal of Hydrology*, *610*, 127879. https://doi.org/10.1016/j.jhydrol.2022.127879

Claessens, L., Hopkinson, C., Rastetter, E., & Vallino, J. (2006). Effect of historical changes in land use and climate on the water budget of an urbanizing watershed. *Water Resources Research*, *42*(3), W03426. https://doi.org/10.1029/2005WR004131

Cohard, J.-M., Rosant, J.-M., Rodriguez, F., Andrieu, H., Mestayer, P. G., & Guillevic, P. (2018). Energy and water budgets of asphalt concrete pavement under simulated rain events. *Urban Climate*, *24*, 675–691. https://doi.org/10.1016/j.uclim.2017.08.009

DeOreo, W. B., Mayer, P. W., Dziegielewski, B., & Kiefer, J. (2016). *Residential end uses of water, version 2*. Water Research Foundation.

Diem, J. E. (2023). Evapotranspiration data for land cover in the South River Watershed (Atlanta, GA, USA) [Dataset]. Retrieved from https://data.mendeley.com/datasets/styx6bjgvj

Diem, J. E., Pangle, L. A., Milligan, R. A., & Adams, E. A. (2021). Intra-annual variability of urban effects on streamflow. *Hydrological Processes*, *35*(9), e14371. https://doi.org/10.1002/hyp.14371

Diem, J. E., Pangle, L. A., Milligan, R. A., & Adams, E. A. (2022). How much water is stolen by sewers? Estimating watershed-level inflow and infiltration throughout a metropolitan area. *Journal of Hydrology*, *614*, 128629. https://doi.org/10.1016/j.jhydrol.2022.128629

Ek, M. B., Mitchell, K. E., Lin, Y., Rogers, E., Grunmann, P., Koren, V., et al. (2003). Implementation of Noah land surface model advances in the National Centers for Environmental Prediction operational mesoscale Eta model. *Journal of Geophysical Research*, *108*(D22). https://doi.org/10.1029/2002JD003296

Fang, D., Hao, L., Cao, Z., Huang, X., Qin, M., Hu, J., et al. (2020). Combined effects of urbanization and climate change on watershed evapotranspiration at multiple spatial scales. *Journal of Hydrology*, *587*, 124869. https://doi.org/10.1016/j.jhydrol.2020.124869

Fang, Y., Sun, G., Caldwell, P., McNulty, S. G., Noormets, A., Domec, J.-C., et al. (2015). Monthly land cover-specific evapotranspiration models derived from global eddy flux measurements and remote sensing data. *Ecohydrology*, *9*(2), 248–266. https://doi.org/10.1002/eco.1629

Gao, J., & O'Neill, B. C. (2020). Mapping global urban land for the 21st century with data-driven simulations and Shared Socioeconomic Pathways. *Nature Communications*, *11*(1), 2302. https://doi.org/10.1038/s41467-020-15788-7

Gash, J. H. C., Rosier, P. T. W., & Ragab, R. (2008). A note on estimating urban roof runoff with a forest evaporation model. *Hydrological Processes*, *22*(8), 1230–1233. https://doi.org/10.1002/hyp.6683

Grimmond, C. S. B., & Oke, T. R. (1991). An evapotranspiration-interception model for urban areas. *Water Resources Research*, *27*(7), 1739–1755. https://doi.org/10.1029/91WR00557

Grimmond, C. S. B., & Oke, T. R. (1999a). Evapotranspiration rates in urban areas. *Proceedings of IUGG 99 Symposium HS5*, *259*, 235–243.

Güneralp, B., Reba, M., Hales, B. U., Wentz, E. A., & Seto, K. C. (2020). Trends in urban land expansion, density, and land transitions from 1970 to 2010: A global synthesis. *Environmental Research Letters*, *15*(4), 044015. https://doi.org/10.1088/1748-9326/ab6669

Gyamfi, C., Ndambuki, J., & Salim, R. (2016). Hydrological responses to land use/cover changes in the Olifants Basin, South Africa. *Water*, *8*(12), 588. https://doi.org/10.3390/w8120588

Hamilton, S. K., Hussain, M. Z., Lowrie, C., Basso, B., & Robertson, G. P. (2018). Evapotranspiration is resilient in the face of land cover and climate change in a humid temperate catchment. *Hydrological Processes*, *32*(5), 655–663. https://doi.org/10.1002/hyp.11447

Hao, L., Huang, X., Qin, M., Liu, Y., Li, W., & Sun, G. (2018). Ecohydrological processes explain urban dry island effects in a wet region, southern China. *Water Resources Research*, *54*(9), 6757–6771. https://doi.org/10.1029/2018WR023002

Hodnett, M. G., da Silva, L. P., da Rocha, H. R., & Cruz Senna, R. (1995). Seasonal soil water storage changes beneath central Amazonian rainforest and pasture. *Journal of Hydrology*, *170*(1–4), 233–254. https://doi.org/10.1016/0022-1694(94)02672-X

Hogan, P., Parajka, J., Oismüller, M., Heng, L., Strauss, P., & Blöschl, G. (2020). High-frequency stable-isotope measurements of evapotranspiration partitioning in a maize field. *Water*, *12*(11), 3048. https://doi.org/10.3390/w12113048

Järvi, L., Grimmond, C. S. B., & Christen, A. (2011). The surface urban energy and water balance scheme (SUEWS): Evaluation in Los Angeles and Vancouver. *Journal of Hydrology*, *411*(3–4), 219–237. https://doi.org/10.1016/j.jhydrol.2011.10.001

Jia, Y., Ni, G., Kawahara, Y., & Suetsugi, T. (2001). Development of WEP model and its application to an urban watershed. *Hydrological Processes*, *15*(11), 2175–2194. https://doi.org/10.1002/hyp.275

Kokkonen, T. V., Grimmond, C. S. B., Christen, A., Oke, T. R., & Järvi, L. (2018). Changes to the water balance over a century of urban development in two neighborhoods: Vancouver, Canada. *Water Resources Research*, *54*(9), 6625–6642. https://doi.org/10.1029/2017WR022445

Lindsey, R. (2021). New maps of annual average temperature and precipitation from the U.S. Climate Normals. *National Oceanic and Atmospheric Administration*. Retrieved from https://www.climate.gov/news-features/featured-images/new-maps-annual-average-temperature-and-precipitation-us-climate

Litvak, E., Manago, K. F., Hogue, T. S., & Pataki, D. E. (2017). Evapotranspiration of urban landscapes in Los Angeles, California at the municipal scale. *Water Resources Research*, *53*(5), 4236–4252. https://doi.org/10.1002/2016WR020254

Liu, W., Hong, Y., Khan, S. I., Huang, M., Vieux, B., Caliskan, S., & Grout, T. (2010). Actual evapotranspiration estimation for different land use and land cover in urban regions using Landsat 5 data. *Journal of Applied Remote Sensing*, *4*(1), 041873. https://doi.org/10.1117/1.3525566

McMahon, T. A., Peel, M. C., Lowe, L., Srikanthan, R., & McVicar, T. R. (2013). Estimating actual, potential, reference crop and pan evaporation using standard meteorological data: A pragmatic synthesis. *Hydrology and Earth System Sciences*, *17*(4), 1331–1363. https://doi.org/10.5194/hess-17-1331-2013

Midcap, J. T., Weatherly, N., & Chappell, M. (2020). *Landscape plants for Georgia. Bulletin 625*. University of Georgia Cooperative Extension. Retrieved from https://secure.caes.uga.edu/extension/publications/files/pdf/B%20625_6.PDF

Mitchell, V. G., McMahon, T. A., & Mein, R. G. (2003). Components of the total water balance of an urban catchment. *Environmental Management*, *32*(6), 735–746. https://doi.org/10.1007/s00267-003-2062-2

Myneni, R., Knyazikhin, Y., & Park, T. (2015). MOD15A2H MODIS leaf area index/FPAR 8-day L4 global 500m SIN grid V006 [Dataset]. NASA EOSDIS Land Processes DAAC. Retrieved from https://modis.gsfc.nasa.gov/data/dataprod/mod15.php

Nagy, R. C., & Lockaby, B. G. (2011). Urbanization in the southeastern United States: Socioeconomic forces and ecological responses along an urban-rural gradient. *Urban Ecosystems*, *14*(1), 71–86. https://doi.org/10.1007/s11252-010-0143-6

Oke, T. R. (1979). Advectively-assisted evapotranspiration from irrigated urban vegetation. *Boundary-Layer Meteorology*, *17*(2), 167–173. https://doi.org/10.1007/BF00117976

Opalinski, N. F., Bhaskar, A. S., & Manning, D. T. (2020). Spatial and seasonal response of municipal water use to weather across the contiguous U.S. *Journal of the American Water Resources Association*, *56*(1), 68–81. https://doi.org/10.1111/1752-1688.12801

Pangle, L. A., Diem, J. E., Milligan, R., Adams, E., & Murray, A. (2022). Contextualizing inflow and infiltration within the streamflow regime of urban watersheds. *Water Resources Research*, *58*(1). https://doi.org/10.1029/2021WR030406

Passarello, M. C., Sharp, J. M., & Pierce, S. A. (2012). Estimating urban-induced artificial recharge: A case study for Austin, TX. *Environmental and Engineering Geoscience*, *18*(1), 25–36. https://doi.org/10.2113/gseegeosci.18.1.25

Peters, E. B., Hiller, R. V., & McFadden, J. P. (2011). Seasonal contributions of vegetation types to suburban evapotranspiration. *Journal of Geophysical Research*, *116*(G1), G01003. https://doi.org/10.1029/2010JG001463

Ragab, R., Bromley, J., Rosier, P., Cooper, J. D., & Gash, J. H. C. (2003). Experimental study of water fluxes in a residential area: 1. Rainfall, roof runoff and evaporation: The effect of slope and aspect. *Hydrological Processes*, *17*(12), 2409–2422. https://doi.org/10.1002/hyp.1250

Ragab, R., Rosier, P., Dixon, A., Bromley, J., & Cooper, J. D. (2003). Experimental study of water fluxes in a residential area: 2. Road infiltration, runoff and evaporation. *Hydrological Processes*, *17*(12), 2423–2437. https://doi.org/10.1002/hyp.1251

Ramier, D., Berthier, E., & Andrieu, H. (2004). An urban lysimeter to assess runoff losses on asphalt concrete plates. *Physics and Chemistry of the Earth, Parts A/B/C*, *29*(11–12), 839–847. https://doi.org/10.1016/j.pce.2004.05.011

Ramier, D., Berthier, E., & Andrieu, H. (2011). The hydrological behaviour of urban streets: Long-term observations and modelling of runoff losses and rainfall-runoff transformation. *Hydrological Processes*, *25*(14), 2161–2178. https://doi.org/10.1002/hyp.7968

Rutsch, M., Rieckermann, J., Cullmann, J., Ellis, J. B., Vollertsen, J., & Krebs, P. (2008). Towards a better understanding of sewer exfiltration. *Water Research*, *42*(10–11), 2385–2394. https://doi.org/10.1016/j.watres.2008.01.019

Sailor, D. J., Georgescu, M., Milne, J. M., & Hart, M. A. (2015). Development of a national anthropogenic heating database with an extrapolation for international cities. *Atmospheric Environment*, *118*(7–18), 7–18. https://doi.org/10.1016/j.atmosenv.2015.07.016

Scott, R. L. (2010). Using watershed water balance to evaluate the accuracy of eddy covariance evaporation measurements for three semiarid ecosystems. *Agricultural and Forest Meteorology*, *150*(2), 219–225. https://doi.org/10.1016/j.agrformet.2009.11.002

Sloto, R. A., & Buxton, D. E. (2005). *Water budgets for selected watersheds in the Delaware river basin, eastern Pennsylvania and western New Jersey (Report No. 2005–5113), Scientific Investigations Report*. United States Geological Survey. https://doi.org/10.3133/sir20055113

Thompson, S. E., Harman, C. J., Konings, A. G., Sivapalan, M., Neal, A., & Troch, P. A. (2011). Comparative hydrology across AmeriFlux sites: The variable roles of climate, vegetation, and groundwater. *Water Resources Research*, *47*(10). https://doi.org/10.1029/2010WR009797

Thornthwaite, C. W. (1948). An approach toward a rational classification of climate. *Geographical Review*, *38*(1), 55–94. https://doi.org/10.2307/210739

Townsend-Small, A., Pataki, D. E., Liu, H., Li, Z., Wu, Q., & Thomas, B. (2013). Increasing summer river discharge in southern California, USA, linked to urbanization. *Geophysical Research Letters*, *40*(17), 4643–4647. https://doi.org/10.1002/grl.50921

Trewartha, G. T., & Horn, L. H. (1980). *An introduction to climate*. McGraw-Hill.

Welty, C. (2009). The urban water budget. In L. A. Baker (Ed.), *The water environment of cities* (pp. 17–28). Springer US. https://doi.org/10.1007/978-0-387-84891-4_2

Williams, C. A., Reichstein, M., Buchmann, N., Baldocchi, D., Beer, C., Schwalm, C., et al. (2012). Climate and vegetation controls on the surface water balance: Synthesis of evapotranspiration measured across a global network of flux towers. *Water Resources Research*, *48*(6). https://doi.org/10.1029/2011WR011586

Winbourne, J. B., Jones, T. S., Garvey, S. M., Harrison, J. L., Wang, L., Li, D., et al. (2020). Tree transpiration and urban temperatures: Current understanding, implications, and future research directions. *BioScience*, *70*(7), 576–588. https://doi.org/10.1093/biosci/biaa055

Woods, A. J., Omernik, J. M., Butler, D. R., Ford, J. G., Henley, J. E., Hoagland, B. W., et al. (2005). Ecoregions of Oklahoma (color poster with map, descriptive text, summary tables, and photographs): Reston, Virginia, U.S. Geological Survey (map scale 1:1,250,000). United States Geological Survey. Retrieved from https://gaftp.epa.gov/EPADataCommons/ORD/Ecoregions/ok/ok_eco_lg.pdf

Zhang, K., & Parolari, A. J. (2022). Impact of stormwater infiltration on rainfall-derived inflow and infiltration: A physically based surface–subsurface urban hydrologic model. *Journal of Hydrology*, *610*, 127938. https://doi.org/10.1016/j.jhydrol.2022.127938

Zhang, L., Dawes, W. R., & Walker, G. R. (2001). Response of mean annual evapotranspiration to vegetation changes at catchment scale. *Water Resources Research*, *37*(3), 701–708. https://doi.org/10.1029/2000WR900325

References From the Supporting Information

Alduchov, O. A., & Eskridge, R. E. (1996). Improved Magnus form approximation of saturation vapor pressure. *Journal of Applied Meteorology*, *35*(4), 601–609. https://doi.org/10.1175/1520-0450(1996)035<0601:IMFAOS>2.0.CO;2

Grimmond, C. S. B., & Oke, T. R. (1999b). Heat storage in urban areas: Local-scale observations and evaluation of a simple model. *Journal of Applied Meteorology*, *38*(7), 922–940. https://doi.org/10.1175/1520-0450(1999)038<0922:HSIUAL>2.0.CO;2

Grimmond, C. S. B., & Oke, T. R. (2002). Turbulent heat fluxes in urban areas: Observations and a Local-Scale Urban Meteorological Parameterization Scheme (LUMPS). *Journal of Applied Meteorology*, *41*(7), 792–810. https://doi.org/10.1175/1520-0450(2002)041<0792:thfiua>2.0.co;2